Published in: Physiological Measurement (2017) vol. 38, p. 397
https://iopscience.iop.org/article/10.1088/1361-6579/aa57b4

Estimation of the QT-RR relation: trade-off between goodness-of-fit and extrapolation accuracy

Alain Vinet [1, 2, 3], Bruno Dubé [2], Réginald Nadeau[2], Omar Mahiddine[2], Vincent Jacquemet[1, 2, 3]

[1] *Department of Molecular and Integrative Physiology, Faculty of Medicine, Université de Montréal, Montréal, QC, Canada.*

[2] *Centre de Recherche, Hôpital du Sacré-Cœur, Montréal, QC, Canada*;

[3] *Institut de Génie Biomédical, Université de Montréal, Montréal, QC, Canada.*

Correspondence:

Vincent Jacquemet
Hôpital du Sacré-Cœur de Montréal
Centre de Recherche
5400 boul. Gouin Ouest
Montréal (Québec) Canada H4J 1C5
phone: +1 514 338 2222 ext. 2522
fax: +1 514 338 2694
vincent.jacquemet@umontreal.ca

Running title

Goodness-of-fit and extrapolation accuracy of the QT-RR curve

Keywords

QT interval, QT correction, QT-RR relation, hysteresis reduction

Abstract

Correction of the QT interval in the ECG for changes in heart rate (RR interval) is needed to compare groups of patients and assess the risk of sudden cardiac death. The QTc represents the QT interval at 60 bpm, although most patients typically have a faster heart rate, thus requiring extrapolation of the QT-RR relationship.

This paper investigates the ability of QT-RR models with increasing number of parameters to fit beat-to-beat variations in the QT interval and provide a reliable estimate of the QTc. One-, two- and three-parameter functions generalising the Bazett and Fridericia formulas were used in combination with hysteresis reduction (memory) obtained by time-averaging the history of RR intervals with exponentially-decaying weights. In normal men and women datasets of Holter recordings in normal subjects (24h monitoring), two measures were computed for each model: the root mean square error (RMSE) of fitting and the difference between the estimated QTc and a reference QTc obtained by collecting data points around RR = 1000 ms.

The two- and three-parameter functions all gave similar low RMSE with uncorrelated residues. An optimal memory parameter was found that still minimized the RMSE and could be used for all functions and subjects. This reduction in RMSE resulted from changes in the parameters linked to the increased steepness of the QT-RR relation after hysteresis reduction. At optimal memory, the two and three-parameter models provided poorer prediction of the QTc as compared to the Fridericia's model in subjects with fast heart rates, since accurate representation of the steeper QT-RR relation worsened the extrapolation that was then needed to determine the QTc. As a result,

among all models investigated, the Fridericia formulation offered the best trade-off for QTc prediction robust to memory and fast heart rates.

Abbreviations

B, F, P	: QT model; Bazett, Fridericia, power optimized
B^{o}, F^{o}, P^{o}	: Bazett, Fridericia, power optimized with offset
QT	: QT interval
JT	: JT interval
QTX	: predicted QT for model X (X = B, F, P, B^{o}, F^{o}, P^{o}, B^{JT}, P^{JT})
QTX_{c}	: corrected QT for model X (X = B, F, P, B^{o}, F^{o}, $P^{o,}$ B^{JT}, P^{JT})
τ	: memory time constant (in beats) of the autoregressive filter
m	: exponent of QT model
K_1, K_2	: regression coefficient of QT model
RR, $\overline{RR}$	: RR interval, raw and with memory
QT^{1}_{ref}	: QT reference at RR = 1000 ms=1 sec
QTX^{1}	: predicted QT at RR = 1000 ms by model X (X = B, F, P…)
M	: Men 24-hour Holter group
W	: Women 24-hour Holter group

1. Introduction

Numerous studies have been devoted to the analysis of the QT vs. RR relationship in time series extracted from ECG recordings (Molnar *et al.*, 1996; Malik *et al.*, 2002; Pueyo *et al.*, 2004; Malik *et al.*, 2008a; Malik *et al.*, 2008b; Halamek *et al.*, 2010; Jacquemet *et al.*, 2011; Cabasson *et al.*, 2012; Pickham *et al.*, 2012). Their aim was either to typify the QT dependency to RR among subjects and conditions, or to obtain a reliable estimate of the QT_c (QT at RR = 1 sec.) to be used for clinical or regulatory purpose (Isbister & Page, 2013; Rabkin & Cheng, 2015). Different functional representations and fitting criteria were considered (Pueyo *et al.*, 2004). In many instances, a set of QT vs. RR functions were fitted, the most performing being retained for each individual recording (Jacquemet *et al.*, 2011). Since QT changes also display hysteresis upon RR variations, weighted time average of the RR has been used to account for the so-called memory effect (Malik *et al.*, 2008a; Malik, 2014).

Our goal is to further investigate the links between memory, the choice of the QT-RR functions, the goodness-of-fit and the accuracy of QT_c prediction. The paper covers the following topics: 1) Analysis of the ability of selected QT-RR functions, incorporating one to three adjustable parameters and weighted average RR corresponding to progressively decaying memory effects (a procedure referred to as hysteresis reduction), to reproduce the beat-to-beat dynamics of the QT intervals; 2) Comparison of the proportional and linear approaches to compute QT_c from these QT-RR functions; 3) Evaluation the accuracy of QT_c prediction by comparison with a benchmark obtained from QT values measured from episodes where the RR was stable around 1000 ms.

The first section of the paper obtains, through the comparison of two alternative methods, a set of reference QT values that will be compared to the QT_c predicted by the different models. Then, we examine whether optimal memory providing minimal QT vs. RR fitting errors should be subject- and/or model-specific. We also investigate whether the improvement of the fitting brought by memory results from specific changes in the values of the parameters and how these are related to the sex of the subjects and the number of adjustable parameters in the models. Finally, two methods to estimate the QT_c are assessed. All these issues are studied in clinical recordings obtained from 24 hours monitoring.

2. Methods

2.1. ECG recordings

ECG signals of a thorough QT study with crossover design (database "Thorough QT Study #2," E-HOL-12-0140-008) were obtained from the Telemetric and Holter ECG Warehouse (THEW, Rochester, NY). 24-hour standard 12-lead Holter ECGs (1000 samples per second) were recorded in 68 normal subjects during placebo delivery (27 women, age: 47.1±7.8, 41 men, age: 39.8±10.8, T-test, $p=0.004$). The recordings were first resampled at 500 Hz and leads VR, V2 and V5 were selected to form an equivalent three-lead system.

2.2. Preprocessing and time series extraction

ECG signals were band-pass filtered (0.01–100 Hz). An ECG fiducial point detector (Dubé *et al.*, 1988) was applied to the magnitude of the signal (RMS of the three ECG leads) to identify the markers Q, R, S and T. The beginning (Q) and end (S) of the QRS were defined as the position corresponding to 2% of the maximum of the R wave before and after the peak value respectively. The marker R was set at the center of gravity of the QRS complex (median of the area between Q and S). The marker T (i.e. end of repolarization) was placed at the intersection of the baseline and the tangent at the steepest negative slope of the lowpass-filtered T wave (15 Hz cutoff frequency) (Xue & Reddy, 1998). QRS, QT and JT intervals were defined as S-Q, T-Q and QT-QRS respectively, and RR as the period between successive R markers. In the sequel, QT(n), QRS(n) and JT(n) refer to the intervals within the n-th beat, and RR(n) to the RR interval from the preceding beat.Markers were validated by examination of the QT and RR time series using a combination of ECG analysis software (Dubé *et al.*, 1988) and Burdick Vision Premier Holter (Cardiac Science, Bothell, WA, USA) operated by experienced operators. After a preliminary automatic analysis, all individual RR and QT time series, as well as the ECG, were examined to remove ectopic beats, compensatory pauses, episodes of arrhythmia and unreliable beats that may have been missed, as well as abnormal QT coming from noisy stretches of recordings. All analyses were performed using the validated time series consisting of normal sinus beats with reliable QT intervals.

2.3. Memory

The response of the QT interval to abrupt changes in heart rate is characterized by a slow adaptation, by which the change of QT lags behind the change of RR. Upon successive increase and decrease of the RR, the QT variation depends on the RR time course and displays hysteresis. This is usually be taken into account by introducing an effective RR interval, denoted by $\overline{\mathrm{RR}}$ and computed from the past RR intervals, which is then used to predict the QT. This is equivalent to filtering the RR time series. This filter may be chosen to be a moving average (Ehlert *et al.*, 1992), a one- or two-parameter transfer function (Halamek *et al.*, 2010; Jacquemet *et al.*, 2011), be subject-specific (Pueyo *et al.*, 2004; Malik *et al.*, 2008a), or QT-RR hysteresis may be simply neglected (Molnar *et al.*, 1996; Rautaharju & Zhang, 2002). We used an autoregressive filter approach that has been extensively validated (Jacquemet *et al.*, 2014; Malik, 2014; Malik *et al.*, 2016) and is defined by the formula:

$$\overline{\mathrm{RR}}(\mathrm{n}) = \mathrm{c}\,\mathrm{RR}(\mathrm{n}) + (1-\mathrm{c})\ \overline{\mathrm{RR}}(\mathrm{n}-1) \quad , \qquad (1)$$

where $0 < c \leq 1$ is the memory parameter. This is equivalent to exponentially decaying weights:

$$\overline{\mathrm{RR}}(\mathrm{n}) = \mathrm{c}\sum_{\mathrm{i}=0}^{\infty}(1-\mathrm{c})^{\mathrm{i}}\mathrm{RR}(\mathrm{n}-\mathrm{i}) = \sum_{\mathrm{i}=0}^{\infty}\mathrm{w}_{\mathrm{i}}\mathrm{RR}(\mathrm{n}-\mathrm{i}) \qquad (2)$$

$$\sum_{\mathrm{i}=0}^{\mathrm{k}}\mathrm{w}_{\mathrm{i}} = 1-(1-\mathrm{c})^{\mathrm{k}+1} \qquad (3)$$

The model therefore discards the instantaneous effect of action potential duration restitution (Franz *et al.*, 1983) on the QT interval in normal subjects during sinus rhythm. Some attention to this additional effect may be needed in the context of arrhythmia, exercise or tilt table test (Cabasson *et al.*, 2012).

The number of preceding beats needed to reach 95% of the total cumulative weight, denoted by $\tau = \max(1, \log(0.05)/\log(1\text{-c}) - 1)$ was used to quantify the memory (Malik, 2014). The memory parameter τ was varied from 1 beat (no memory, c = 1) to

500 beats (long memory, c $\cong$ 0.006). For the sake of convenience, $\overline{RR}$ was divided by 1000 ms to provide non-dimensional normalized time series.

2.4. QT models

The Bazett's and Fridericia's formulas are the standard clinical representation of the QT vs $\overline{RR}$ relationship:

$$\begin{aligned} \text{Bazett (model B)}: \quad & \mathrm{QTB}(n) = K_2 \cdot \overline{\mathrm{RR}}(n)^{1/2} \\ \text{Fredericia (model F)}: \quad & \mathrm{QTF}(n) = K_2 \cdot \overline{\mathrm{RR}}(n)^{1/3} \end{aligned} \quad ,$$

in which QTB(n) and QTF(n) refer to the beat-to-beat predicted QT by each function. In this article, we chose to include the simplest extensions of these functions by allowing the exponent of the RR to vary and/or by adding an offset. In the sequel, we referred to these functions as models. The most general model, denoted by P^O (adaptive power (P) with offset (o)) is expressed as:

$$\text{model} \quad P^O: \quad \mathrm{QTP}^O(n) = K_1 + K_2 \cdot \overline{\mathrm{RR}}(n)^m \qquad (4)$$

where K_1, K_2 and m are parameters to be adapted to each subject.

Additional models were created by applying the functions to the JT interval instead of the QT interval (Tsai *et al.*, 2014). Since QRS duration only depends weakly on heart rate (5 to 8 ms variation for full RR range (Malik *et al.*, 2008b)) and its beat-to-beat determination is commonly less accurate than the QT, the JT time series was defined as $\mathrm{JT}(n) = \mathrm{QT}(n) - \langle \mathrm{QRS} \rangle$, where $\langle \mathrm{QRS} \rangle$ was the mean QRS duration over the whole recording. Predicted QT values were then recovered by adding the subject-specific

$\langle QRS \rangle$ to the predicted JT. This was done for the B and P model (B^{JT},P^{JT}). The results of the F^{JT} were the poorest among all models and are not presented. The effect of memory was also taken into account by fitting the models with $\overline{RR}$ computed from a large set of c values

The B^{JT} and P^{JT} models are equivalent to setting the parameter K_1 of the B^o and P^o model to the subject-specific $\langle QRS \rangle$. There were introduced to test whether the K_1 parameter obtained by the fit was close to $\langle QRS \rangle$. The eight different models are summarized in Table 1.

Model	Nb. of Parameters
$B: \quad QTB(n) = K_2 \cdot \overline{RR}(n)^{1/2}$	1
$F: \quad QTF(n) = K_2 \cdot \overline{RR}(n)^{1/3}$	1
$B^{JT}: \quad QTB^{JT}(n) = \langle QRS \rangle + K_2 \cdot \overline{RR}(n)^{1/2}$	1
$P: \quad QTP(n) = K_2 \cdot \overline{RR}(n)^{m}$	2
$P^{JT}: \quad QTP^{JT}(n) = \langle QRS \rangle + K_2 \cdot \overline{RR}(n)^{m}$	2
$B^o: \quad QTB^o(n) = K_1 + K_2 \cdot \overline{RR}(n)^{1/2}$	2
$F^o: \quad QTF^o(n) = K_1 + K_2 \cdot \overline{RR}(n)^{1/3}$	2
$P^o: \quad QP^o(n) = K1 + K_2 \cdot \overline{RR}(n)^{m}$	3

Table I: The eight models and their number of parameters.

Fitting was performed for each subject using an iterative least square method implemented in Matlab (nlinfit). To secure convergence in the three parameters P^O model, the K_1 and K_2 parameters were first estimated from two-parameter optimization with *m* varying from -3 to 3 by step of 0.04. The variant with minimum residue was picked as initial condition for the final three-parameter optimization. Analysis was restricted to these models generalizing Bazett's and Fridericia's formula to allow for a comprehensive comparison of the parameters values between models as well as with respect to memory.

The quality of the fits was assessed by the root mean square error (RMSE). Fitting does not necessarily reduce the dispersion of the QT around each RR value. A dispersion index was obtained for each subject by computing the QT standard deviation in successive RR bins of 40 ms width, ranging from 460 to 1400 ms. The dispersion index was calculated for each bin containing at least 40 beats.

2.5. QT correction

A single value for the QTc can be obtained by evaluating the fitted QT-RR relation at $\overline{\mathrm{RR}} = 1$. The resulting value was noted as QTX^1 for the model X, X standing for P, P^O, B, F, etc. However, when QT_c has to be monitored over time, its beat-to-beat evaluation is needed. It can be obtained through two types of formulations, referred to as proportional and linear scaling by Rautaharju and Zhang (2002). The proportional evaluation (index p) is computed as

$$QTX_{cp}(n) = \frac{QT(n)}{\overline{RR(n)}^{m}} + K_1 \cdot \left(1 - \frac{1}{\overline{RR(n)}^{m}}\right) \quad . \tag{7}$$

In the absence of offset (K_1=0), a standard Bazett-like formula is obtained that still required fitting if m is a free parameter. The offset introduces a rate-dependent correction factor in the QT_c estimation. The linear correction (index L) is formulated as

$$QTX_{cL}(n) = \left(QT(n) - K_2 \cdot \overline{RR(n)}^{m}\right) + K_2 \tag{8}$$

The mathematical derivation of the expected values of the mean and standard deviation of $QTX_{cp}(n) - QTX^{1}$ and $QTX_{cL}(n) - QTX^{1}$ are given in Appendix I.

2.6. Reference value for the QT_c

In order to quantify the accuracy of the models at predicting the QT_c, a reference estimate of the QT at RR=1000 ms is desirable. Ideally, it would be the QT interval measured after a long period at a stable RR of 1000 ms (QT^{1}_{ref}), but such stable episodes were rarely present in the recordings. Two algorithms were developed to estimate QT^{1}_{ref}.

The principle of the first algorithm was to select the QT intervals from time windows in which the RR remained within a limited range around 1000 ms. The method had two parameters: (1) ΔRR, the acceptable range (ΔRR = 35 or 50 ms); (2) W, the duration of the window (W = 10 to 120 s by step of 10 s). For each segment of duration W, the mean ($\mu_{RR}(\Delta RR;W)$) and standard deviation ($\sigma_{RR}(\Delta RR;W)$) of RR intervals were calculated. Windows were kept if the interval $\mu_{RR} \pm \sigma_{RR}$ and at least 90% of the RR were within the interval 1000 ± ΔRR. The whole recording was scanned by steps of W/2, and the mean QT value ($\mu_{QT}(\Delta RR;W)$) was calculated for each acceptable window. The window-based estimated of QT^{1}_{ref}, denoted by $QT^{1}_{ref,W}$, was computed as the average of the $\mu_{QT}(\Delta RR;W)$ overall values of ΔRR and W. This method puts more weight on long stable intervals, since they contribute to multiple windows.

In the second algorithm, the RR time series was filtered by a series of autoregressive filters as in Eq. (1) with c = [1.5, 2, 2.5, 3, 4, 5, 7, 10, 25, 50] × 10^{-2}. For each value of c, the QT of all beats for which the filtered RR was within the [975, 1025] ms range were averaged, giving an estimate $QT^{1}_{ref,AR}(c)$. The final estimate $QT^{1}_{ref,AR}$ was taken as the average of $QT^{1}_{ref,AR}(c)$ over all values of c.

The two estimates $QT^{1}_{ref,AR}$ and $QT^{1}_{ref,W}$ were compared using pair Student T-test (equality of mean), F-test (equality of variance), Bradley-Blackwood test (equality of mean and variance together) and Lin concordance coefficient.

2.7. Comparison of QT^{1}_{ref} with QT_c

QT^{1}_{ref} and QT_c predicted by the different models were compared through repeated-measure Anova, using Huynh-Feldt correction for significance.

3. Results

3.1. Reference QT interval at 1000 ms

As expected (Stramba-Badiale *et al.*, 1997; Malik *et al.*, 2013), $QT^{1}_{ref,\,AR}$ and $QT^{1}_{ref,\,W}$ were both longer in women than in men ($p < 0.001$ for both, Table 2). For men (M), there were no significant differences between the two measures. For women (W), there was a tendency for $QT^{1}_{ref,\,AR}$ to be slightly longer ($QT^{1}_{ref,\,AR}$ - $QT^{1}_{ref,\,W}$, $p=0.01$, 95% confidence interval: 0.28-2.24 ms), but they nevertheless had a very high level of concordance. A shortcoming of the window method, beside its complexity, was that $QT^{1}_{ref,\,W}$ could not be calculated in one woman who had no acceptable window. Hence, $QT^{1}_{ref,\,AR}$ was chosen as QT^{1}_{ref} for further analysis. No QT^{1}_{ref} was above the values that have been proposed as clinical threshold for long QT_c (Hofman *et al.*, 2007).

	Men	Women
n	41	26
$QT^1_{ref,AR}$ $(\mu_{AR} \pm \sigma_{AR})$	373.0 ± 14.1 ms	401.9 ± 15.7 ms
$QT^1_{ref,W}$ $(\mu_{W} \pm \sigma_{W})$	372.9 ± 13.2 ms	400.6 ± 15.7 ms
$QT^1_{ref,AR} - QT^1_{ref,W}$	0.04 ± 3.36 ms	1.26 ± 2.42 ms
Prob $(\sigma_{AR} = \sigma_{W})$	0.67	0.99
Prob $(\mu_{AR} = \mu_{W})$	0.94	0.01*
B-B	1.64	3.37
Prob (B-B)	0.21	0.05*
$\rho(\mu_{AR} - \mu_w, \mu_{AR} + \mu_w)$	0.29	>-0.001
Prob $(\rho = 0)$	0.08	0.99
ρ_{cc}	0.97	0.98

Table 2: Comparison of $QT^1_{ref,AR}$ and $QT^1_{ref,W}$ in each group. Prob: probability of the null hypothesis for each test. B-B: Bradley-Blackwood test; ρ : correlation between the sum and difference of the two values; ρ_{cc} : Lin's concordance coefficient.

3.2. Goodness-of-fit of the QT-RR relation

This section examines the ability of the different models to reproduce QT vs RR variations. Two questions are investigated:

1) Using the fitting root-mean-square error (RMSE) as a yardstick, was there an optimal memory τ providing the best fit, and was this optimal memory specific to both subjects and models? We conclude that an optimal τ can be used for all models and all subject.

2) Was memory associated to a change of the values of the parameters of the models? We show that the answer depends on the number of parameters of the models.

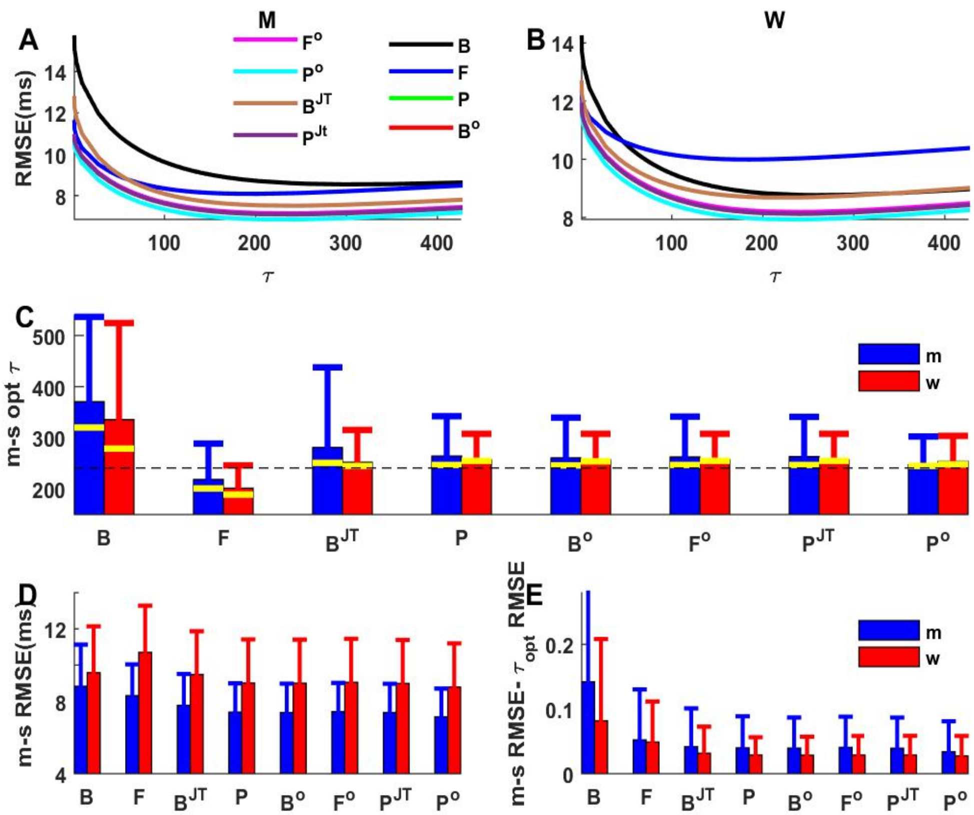

Fig 1. A,B: $\overline{\text{RMSE}}$ of the models as a function of memory in men (M) and women (W). Note that the four 2-parameter models P, P^{JT}, B^{o} and F^{0} are superimposed. **C**: Distribution of the model-subject optimal memory. The yellow lines are the position of the minimum $\overline{\text{RMSE}}$ for each model from panels A and B, the dash line the value of τ_{opt}. **D:** Distribution of the model-subject optimal memory RMSE. **E**: Distribution of the differences between the model-subject optimal memory RMSE and the RMSE using τ_{opt} for all models and subjects.

Effect of memory

Figs 1 A,B show $\overline{\text{RMSE}}$, the RMSE of each model averaged among subjects, as a function of the memory parameter τ for the M and W group respectively. In these, as well as in the curves for each subject (not shown), there was a minimum located as far as 20 ms below the RMSE without memory. It is also noteworthy that curves of all 2-parameters models are superimposed.

The details of the subject-model-optimal τ (τ giving minimum RMSE for each subject and each model) are presented in Fig. 1(c). The B and F models had respectively the longest and shortest subject-optimal τ for both sexes. Women had shorter mean values, except for the P^o model, in agreement with the results obtained by Malik for the Fridericia model (Malik *et al.*, 2016). Still, these sex differences did not reached statistical significance (t-test, $p > 0.25$ for all models). This was substantiated by a Repeated Measures Anova (model*sex), which diagnosed a significant differences only between the models (model, $p < 0.001$), which vanished when the B and F models were discarded ($p = 0.31$). This suggested that the same subject-optimal τ can be used for all models, except possibly for the B and F models.

Besides, the variation of $\overline{\text{RMSE}}$ and of the individual RMSE vs τ were very shallow around their minimum. To quantify RMSE sensitivity to τ, we calculated for each model and subject, the interval $\Delta\tau(\text{Subj},\text{Model}) = \{\tau_{\max} - \tau_{\min}\}$ over which RMSE ≤ min(RMSE(Subj,Model))+0.25ms. All $\Delta\tau(\text{Subj},\text{Model})$ were over 75 beats, the mean values lying around 200 beats for each model, being even larger for the B model. There were no $\Delta\tau(\text{Subj},\text{Model})$ differences between M and W (Anova Sex*model, Sex: p=0.66, Sex*Model: p=0.42). Such a large gap enabled to select a single optimal τ for all subjects and models. In order to remain close to a minimum for all models taken together, we chose τ_{opt} = 241 beats, close to the median of all model-optimal τ obtained from Fig. 1A,B.

Fig 1E displays the distribution of RMSE(Subj,Model)-RMSE(τ_{opt}), which remained much below 0.25 ms except for a few subjects with the B and F models (max: model B: 0.64 ms; F=0.42 ms). The robustness of the F model was conspicuous since the changes of RMSE from subject-optimal τ to τ_{opt} were minimal even if the former was in general shorter than $\tau_{opt.}$

In summary, it is possible to use a single τ_{opt} for all subjects and model, with large latitude in the exact choice. This reconciles our results with those of Malik *et al.* (2013) who reported an average QT/RR hysteresis of 113±16 sec (or 150±21beats for heart rate at 80 bpm) for 14 hour recordings in a large population of healthy subjects.

Model	B	F	B^{JT}	P	B^{O}	F^{O}	P^{JT}	P^{0}
$\overline{\mathrm{RMSE}} \pm \sigma(\mathrm{RMSE})$ **ms, No memory (τ=1) ,**								
M σ±μ	15.7 ± 3.8	11.6 ± 2.2	12.7. ± 2.7	10.9 ± 1.7	10.8 ± 1.7	10.9 ± 1.7	10.8 ± 1.7	10.6 ± 1.6
W σ±μ	14.2 ± 2.5	12.3 ± 2.2	12.6 ± 2.2	11.9 ± 2.2	11.9 ± 2.2	11.9 ± 2.2	11.9 ± 2.2	11.8 ± 2.2
Pr(M=W)	0.14	0.11	0.67	0.03	0.03	0.03	0.03	0.01
τ_{opt} ,								
M σ±μ	8.6 ± 2.2	8.1 ± 1.6	7.5 ± 1.5	7.1 ± 1.4	7.1 ± 1.4	7.1 ± 1.4	7.1 ± 1.4	6.8 ± 1.3
W σ±μ	8.8 ± 1.6	10.0 ± 2.1	8.7 ± 1.5	8.1 ± 1.5	8.1 ± 1.5	8.2 ± 1.5	8.1 ± 1.5	7.9 ± 1.4
Pr(M=W)	0.25	<0.001	0.002	0.001	0.001	0.001	0.001	0.001
RMSE(τ=1)-RMSE(τ_{opt}**)**								
M σ±μ	7.1 ± 2.5	3.4 ± 1.5	5.2 ± 1.9	3.7 ± 1.3	3.7 ± 1.2	3.7 ± 1.2	3.8 ± .1.3	3.8 ± 1.2
W σ±μ	5.4 ± 1.7	2.3 ± 0.9	4.0 ± 1.4	3.7 ± 1.3	3.7 ± 1.2	3.7 ± 1.2	3.8 ± 1.3	3.8 ± 1.4
Pr(M=W)	0.002	<0.001	0.002	0.94	0.92	0.92	0.92	0.96

Table 3: Mean and standard deviation of RMSE without memory and at τ_{opt}. Probability of Kruskal-Wallis test for equality RMSE in the two groups. The last line is the probability that RMSE(τ=1**)-** RMSE(τ_{opt}) was the same in the two groups

Fitting accuracy

The performance of the models could be ranked by their RMSE (Fig. 1D, Table 3). The error was larger for the B, B^{JT} and F model, which was expected since they had only one parameter. A striking feature is the quasi equivalence of all the two and three-parameter models:

- Their RMSE, both without memory and with τ_{opt}, differed only at or beyond the first decimal within each group;

- Their decrease of RMSE at τ_{opt} was the same, and identical in the two groups.

Finally it is also noteworthy that for all models except B, at τ_{opt}, women's RMSE were up to 2 ms larger than men ($p \leq 0.002$). This difference can be explained by the QT vs RR Dispersion Index (Fig. 2), whose mean value remains systematically higher for women.

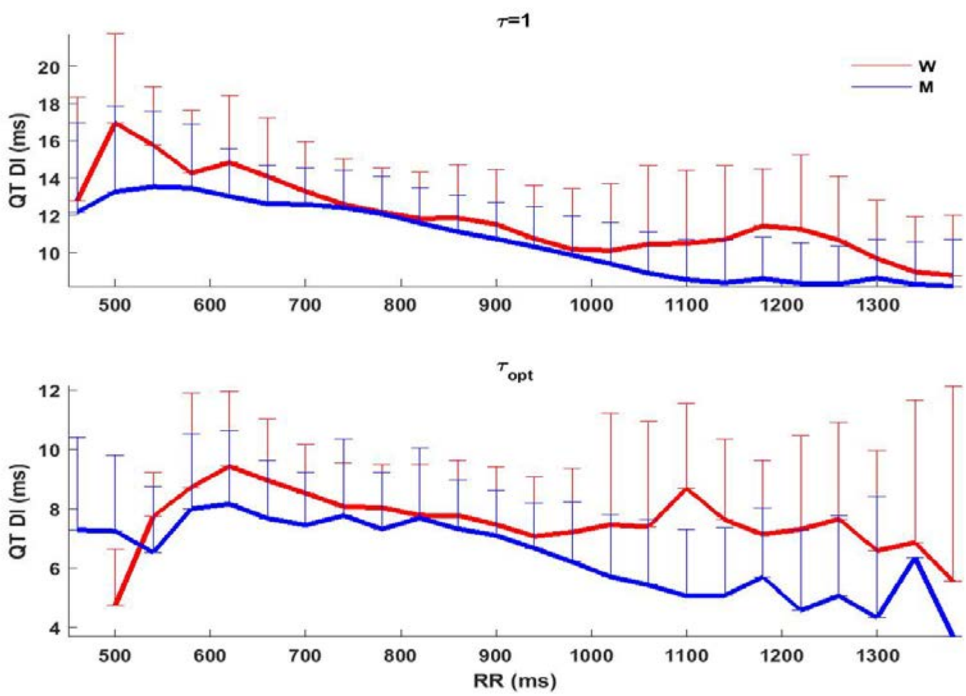

Fig. 2 QT vs RR dispersion without memory (top) and with τ_{opt} (bottom), Women (Red), Men (Blue).

.

	W	M	Prob(M=W)
μ(RR)	882 ± 113	891 ± 79	0.733
$\sigma(\mathrm{RR}(\tau = 1))$	125 ± 27	139 ± 27	0.032
$\sigma(\mathrm{RR}(\tau = 1)) / \mu(\mathrm{RR})$	0.14 ± 0.02	0.16 ± 0.03	0.028
$\sigma(\mathrm{RR}(\tau_{\mathrm{opt}}))$	106 ± 25	113 ± 25	0.155
$\sigma(\mathrm{RR}(\tau_{\mathrm{opt}})) / \mu(\mathrm{RR})$	0.12 ± 0.02	0.13 ± 0.03	0.226
$\sigma(\mathrm{RR}(\tau_{\mathrm{opt}})) / \sigma(\mathrm{RR}(\tau = 1))$	0.85 ± 0.05	0.81 ± 0.07	0.066
μ(QT)	384 ± 22	358 ± 19	<0.001
$\sigma(\mathrm{QT})$	21.7 ± 4.9	19.5 ± 4.4	0.038
$\sigma(\mathrm{QT})/\sigma(\mathrm{RR}(\tau = 1))$	0.18 ± 0.03	0.14 ± 0.03	<0.001
$\sigma(\mathrm{QT})/\sigma(\mathrm{RR}(\tau_{\mathrm{opt}}))$	0.21 ± 0.03	0.17 ± 0.03	<0.001

Table 4: Distribution of Mean $(\mu(\mathrm{QT}), \mu(\mathrm{RR}))$ and standard deviation $(\sigma(\mathrm{QT}), \sigma(\mathrm{RR}))$ of QT and RR, the later calculated without memory $(\tau = 1)$ and at τ_{opt}. Means were compared using T-Test, and the other indices with Kruskal-Wallis Test

Effect of Memory on RR distribution

To grasp the effect of memory, we compared the standard deviations (σ) of the RR intervals without memory and at τ_{opt}. There was a wide variation of μ(RR) and $\sigma(RR(\tau = 1))$ in both groups, with σ/μ ranging from 0.10 to 0.18 (W) or .24 (M) (Table 4). $\sigma(RR(\tau = 1))$ and μ were positively correlated only in women (W: ρ = 0.75, $p < 0.001$; M: ρ = 0.19, p = 0.24). Memory unmistakably reduced σ(RR), on average 15% in women and 19% in men.

Effects of Memory on fitting parameters and residues

Memory can reduce the RMSE by lessening the dispersion of the QT around an invariant QT vs RR relations. Larger $\sigma(\mathrm{QT})/\sigma(\mathrm{RR})$, as seen in women relative to men and τ_{opt} compared with $\tau = 1$, also hints toward steeper QT vs RR slopes and a change of parameters. The correlations of the residues ($\varepsilon(n) = QT(n) - QTX(n)$) with $\overline{RR}^m$, which provide an additional measure of the accuracy, are also considered to assess the quality of the models.

One-parameter models (B, F, B^{JT})

K2	B, $\tau = 1$	B, τ_{opt}	F, $\tau = 1$	F, τ_{opt}	B^{JT}, $\tau = 1$	B^{JT}, τ_{opt}
W	407.3 ± 15.1	408.5 ± 15.1	399.9 ± 13.6	400.5 ± 13.6	341.6 ± 13.0	342.6 ± 13.1
M	377.1 ± 14.3	378.3 ± 14.4	371.3 ± 14.4	371.8 ± 14.5	306.7 ± 13.3	307.6 ± 13.4
Prob B-F	s <0.001, Model: <0.001, Memory: <0.001, Model*Sex: 0.37 Memory*Sex:0.66					
B^{JT}	s <0.001 Memory: <0.001 Model*Sex: 0.68					

Table 5, Value of K2 for the B, F and BJT model, without memory ($\tau = 1$) and at τ_{opt}. Prob are the probability of the different effect in the Sex*Model*Menory repeated measure Anova for B and F model, and Sex*Menory for the B^{JT} model

As seen in table 5, K_2, the only free parameter of these models, was higher in women, which contributes their larger QT dispersion. However, it remained virtually invariant as a function of memory: $0 < \max\left(K_2(\tau_{opt}) - K_2(\tau = 1)\right) \leq 3\,\mathrm{ms}$ for the three models among all subjects. Nevertheless, since $K_2(\tau_{opt}) > K_2(\tau = 1)$ in all cases, there was a similar small but systematic increase of the slope for both sexes. Therefore, RMSE reduction by memory relied essentially on the lessening of the RR dispersion. This is comforting regarding the clinical use of these models, since K_2 was insensitive to the use of raw or weighted RR. The behavior of the B^{JT} model highlighted the shortcoming of the models with fixed exponent without offset. The JT is the QT shifted by a constant, such that the slope of JT vs RR and QT vs RR should by the same. K_2, which corresponds the value of the JT at RR=1, was obviously lower but also brought a systematic reduction of the slope at all RR values.

As seen in Fig. 3, there was a wide dispersion of residue (ε) vs RR^m correlations $\left(\rho\left(\varepsilon, RR^m\right)\right)$ that was not reduced by memory, although correlations were shifted upwards. As shown in Appendix I, this is a consequence of the absence of the parameter K_1 that does not guarantee a null mean value of ε. Hence, the no-correlation criterion of fitting accuracy was not fulfilled in most subjects.

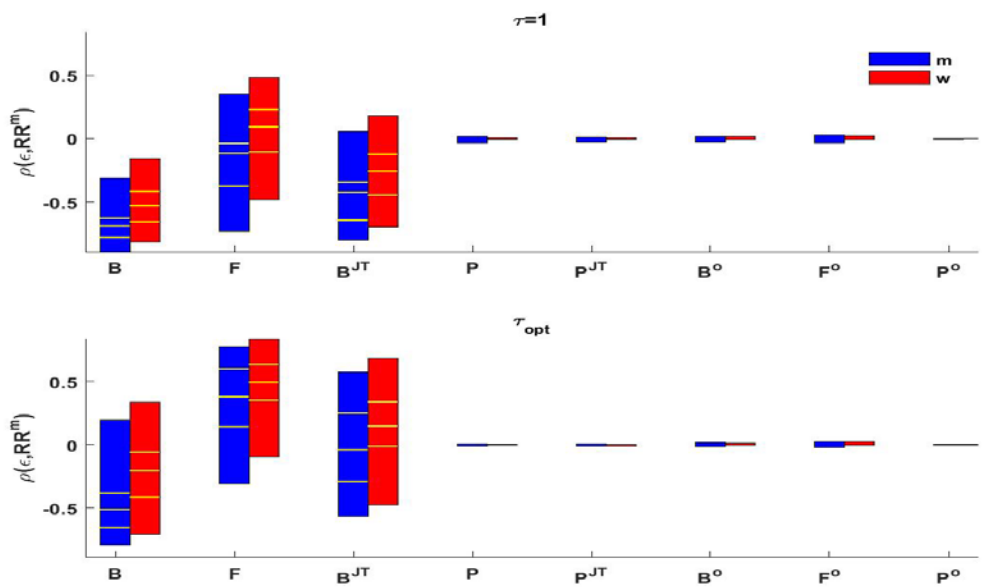

Figure 3: Distribution of the correlation between the residues and RR^m for the different models without memory (top) and τ_{opt} (bottom) for M (blue) and W (red) group. The boxes cover the entire range of correlation, and the yellow lines show the median and first and third quartiles.

The B model had negative correlations, indicating a systematic tendency to overestimate the QT at high RR values both without and at optimal memory (since $\varepsilon(n) = QT(n) - QTB(n)$). The B^{JT} model had a similar trend at low memory, but the center of the distribution was shifted toward 0 at optimal memory. It is noteworthy that even if the B^{JT} model gave low RMSE (Fig. 1), its ε vs. $RR^{1/2}$ correlations were often substantial. The F model with optimal memory had rather the inverse trend to underestimate the QT at high RR.

In summary, memory did not influence the value of the parameter of these models, but changed the distribution of the residues. For the three models, there were many instances of large ε vs. RR^m correlations in the W and M groups, impacting the quality of the prediction at either low or high RR values. This was also the case of B^{JT}, even if it gave low RMSE.

The power models without offset (P and P^{JT})

Since the two models gave similar results, only the P model is presented. Table 6 summarizes the results for τ=1 and τ_{opt}.

		m	K_2 (ms)	$\rho(\varepsilon, \mathrm{RR}^{\mathrm{m}})$	RMSE(ms)
$\tau = 1$	W	0.35 ± 0.06	401.7 ± 16.3	0.001 ± 0.003	11.89 ± 2.18
	M	0.30 ± 0.06	370.8 ± 15.4	0.003 ± 0.007	10.86 ± 1.71
τ_{opt}	W	0.45 ± 0.06	407.2 ± 17.0	0.001 ± 0.002	8.15 ± 1.47
	M	0.40 ± 0.06	375.4 ± 14.9	0.002 ± 0.004	7.11 ± 1.37
Prob	S	<0.001	<0.001	0.88	0.03, <0.001
	τ	<0.001	<0.001	0.29	
	S* τ	0.53	0.41	0.95	0.95

Table 6. P model: Distribution of exponents (m) , K_2, $\rho(\varepsilon, \mathrm{RR}^{\mathrm{m}})$, RMSE for the P and P^{JT} models without memory (τ=1) and at optimal memory (τ_{opt}). The last row gives the significance of the sex (S), memory (τ) and interaction (S* τ). For m, K_2 and ρ: S* τ repeated measure Anova. For ρ, the transformed variable $0.5\ln((1+\rho)/(1-\rho))$ was used for the test. RMSE were compared using Kruskall-Wallis test. First line: S effect for each memory ($\tau = 1, \tau_{opt}$), last line: $\mathrm{RMSE}(\tau = 1) - \mathrm{RMSE}(\tau_{\mathrm{opt}})$.

The parameters m and K_2 were higher in W than M (p < .001), but memory brought similar increase in both groups (p ≥ 0.41), as well as equivalent RMSE reduction (p=0.95). The rise of these parameters increases the range of predicted QT and the mean slope of the QT vs RR function. Hence mean slope was larger in women. It was heightened by memory since it shifts the $\overline{\mathrm{RR}}$ values toward the mean for short runs of low and high RR. As also seen in Fig 3, $\rho(\varepsilon, \mathrm{RR}^{\mathrm{m}})$ was suppressed in these models, even if the parameter K_1 was absent.

Figure 4 shows the behavior of the P model as a function of m. Each subject had an exponent giving a minimum RMSE that was also recovered by fitting directly the two parameters. Hence, for the best exponent, the result is equivalent to a standard least-square fit of QT vs $\overline{RR}^{m_{best}}$. These optimal exponents were distributed over an interval of ~0.25, as broadly scattered in both groups (Fig. 4, M: green line, W: red line,). However, for each subject, there was an interval of about ± 0.1 around its optimal m over which the variation of RMSE was less than 0.5 ms. Considering only RMSE, this would suggest that the same exponent could be used for all subjects without much consequence. For τ=1, the exponent would be close to the 1/3 Fridericia's value for both models, while at τ_{opt}, it would be near the 1/2 Bazett's exponent for the P^{JT} model (not shown).

However, as seen in the middle column panels of Fig. 4, the variation of the ε vs RR^m correlations around the individual optimum m value was much steeper. The correlations at optimal m were low both at τ=1 and τ_{opt} (Fig. 3, Table 3), but varied steeply from positive to negative values as m increased. Exponents lower or higher than the optimal value tended respectively to under- or overestimate the QT at high RR. This also explains the distribution of the correlations for the B, F and B^{JT} models shown in Fig. 2. In conclusion, finding the individual best exponent was needed to reduce the residues, but above all to minimize their correlations with $\overline{RR}^{m}$.

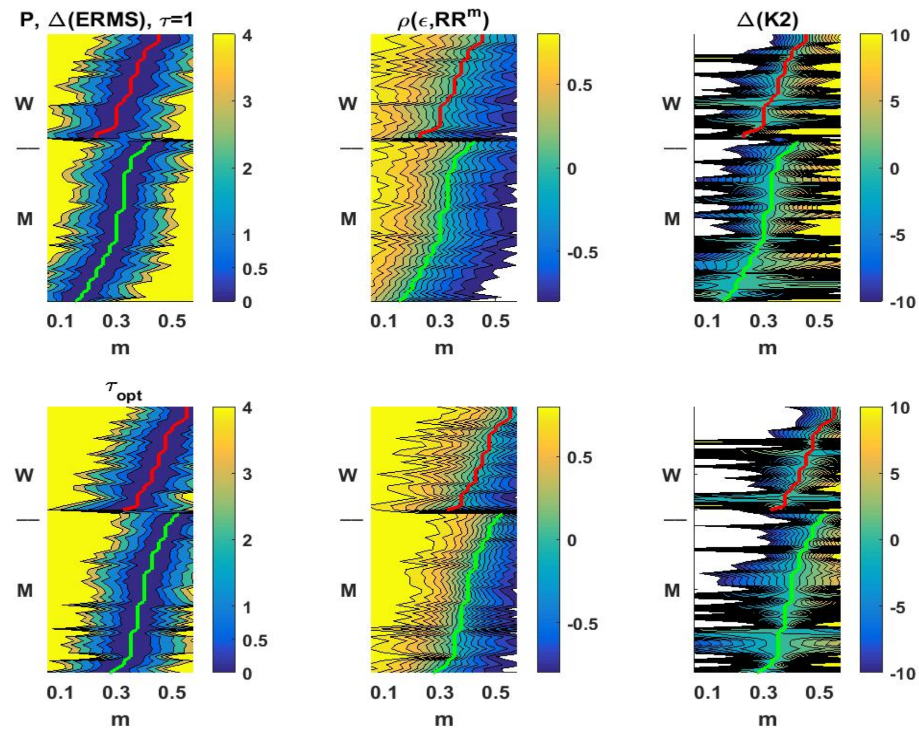

figure 4: P models, without memory (upper panels) and at τ_{opt} (lower panels). In each panel, men (M) are the bottom and women (W) at the top. Subjects were ranked in each group by the value of m giving the minimum of RMSE. **Left column panels:** $\Delta(\mathrm{RMSE})$ = RMSE(m)-min(RMSE). The green and red line indicated, for each subject the best value of m for M and W respectively contour curves correspond to the levels indicated on the ordinate of the colorbar at the right. **Middle panels**: correlation of the residue (ε) and RR^m. Contour curves are from -0.8 to 0.8 by steps of 0.1. **Righ panels:** $\Delta(\mathrm{K2})$ = K2(m)- K2(best m). Contour curves are from -10 to 10 by steps of 1.

Two-parameter models with offset (B^o and F^o)

As seen in Fig. 1, the RMSE of these models were as low as the other two or three parameter models, the offset ensuring no correlation between residues and $RR^{1/2,1/3}$. For all subjects, there was a perfect -1 correlation between $K_1(\tau)$ et $K_2(\tau)$, K_1 and K_2 respectively decreasing and increasing with τ. As aforementioned, memory tends to increase the slope of the QT vs RR relation. In the B, B^{JT} and F models lacking offset, K_2 was the only parameter to increase the slope, but its rise would also shift upward all predicted QT. The decrease of the RMSE that could be obtained through an increase of K_2 was less than the increase associated with the upward shift, in such a way that the fit was always converging toward the same value of K_2, irrespective of memory. In the B^o and F^o models, the K_2-driven upward shift was corrected by a decrease in K_1. However as seen in Table 7, memory brought a huge change of the parameter values. Besides, K_1 was in general far from the mean QRS (M: 41.5 ± 55.4 ms, W: 33.6 ± 42.2 ms), such that the B^0 and F^o model were not equivalent to the B^{JT} and F^{JT}

Despite the huge variations of K_1 and K_2 upon memory, the increase of K_1+ K2, which is the predicted QT at RR=1, was small but highly significant ($p < 0.001$), being similar for the two groups and the two models (Sex* τ : p=0.50, Model*Sex* τ **:** 0.16).

	W				**M**			
(ms)	K_1	K_2	K_1+K_2	$\left\|K_1 - \overline{QRS}\right\|$	K_1	K_2	K_1+K_2	$\left\|K_1 - \overline{QRS}\right\|$
$\mathbf{B^o}$ $\tau = 1$	112.1 ± 46.6	289.8 ± 56.9	401.8 ± 16.2	57.5 ± 36.5	145.9 ± 48.5	225.0 ± 51.3	370.8 ± 15.4	79.5 ± 45.9
$\mathbf{B^o}$ τ_{opt}	35.6 ± 47.1	371.5 ± 59.9	407.1 ± 16.9	42.2 ± 32.7	70.4 ± 43.1	305.0 ± 47.2	375.4 ± 14.9	33.6 ± 25.3
$\mathbf{F^o}$ $\tau = 1$	-21.2 ± 69.1	422.8 ± 80.1	401.6 ± 16.2	90.4 ± 59.6	42.2 ± 69.5	328.6 ± 73.3	370.8 ± 15.4	61.3 ± 38.0
$\mathbf{F^o}$ τ_{opt}	-135.0 ± 71.4	541.6 ± 84.1	406.7 ± 16.7	197.1 ± 71.4	-70.6 ± 62.4	445.8 ± 67.3	375.2 ± 14.9	137.7 ± 61.5
P	Sex: <0.001 , Model : <0.001, Model*Sex: 0.02, τ **:** <0.001, Sex* τ =0.50, Model*Sex* τ **:** 0.16							

Table 7. Distribution of K_1 and K_2 parameters, and of the absolute value of K_1 minus the mean QRS for the B^o at F^o model at $\tau = 1$ and τ_{opt}**.** The last line is the significance of the effects of the Sex*Model*Memory Anova on K_1+ K_2

The three-parameter model (P^0)

The three-parameter P^0 model barely decreased the RMSE as compared to two-parameter models (P^0 vs B^o, F^0 and P models, RMSE difference < 1 ms across all subjects, memory and models). It thus appears superfluous to introduce an extra parameter to get such a tiny improvement of the fit at any value of τ.

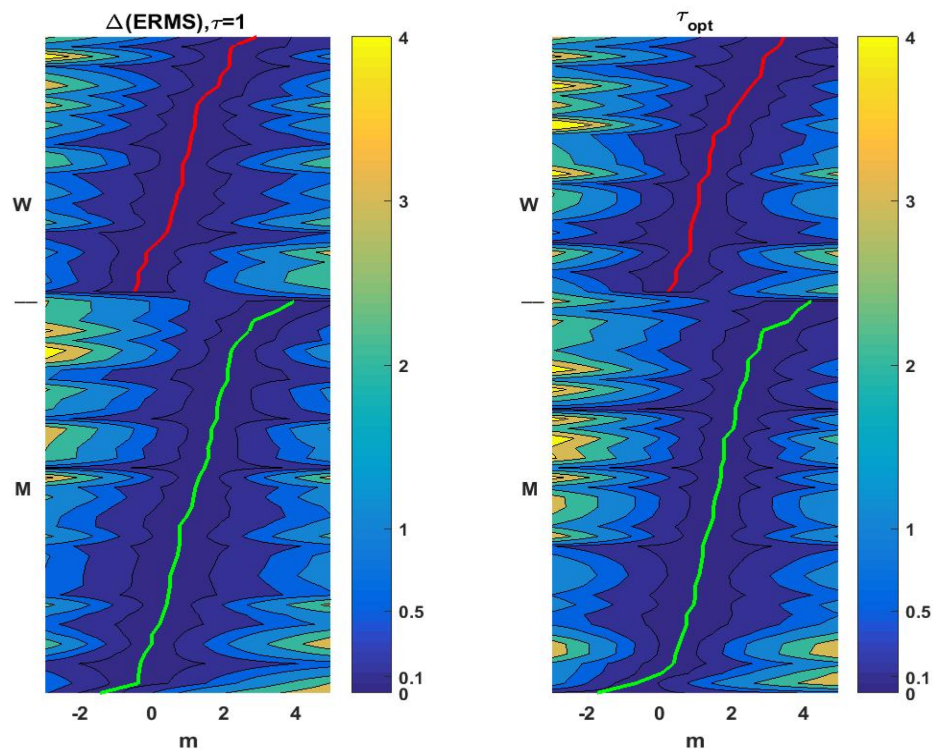

Figure 5: P^o model without memory (left panel) and with τ_{opt} (right panel). RMSE-min(RMSE) (ms) as a function of m for each subject. In each panel, men (M) are at the bottom and women (W) at the top. Subjects were ranked in each group by the value of m giving the minimum of RMSE. Contour curves correspond to the levels indicated on the ordinate of the colorbar at the left of each panel. Green and red line: position of min(ERMS) for M and W subjects respectively.

The variations of the parameters were very large. Fig. 5 shows, for each subject, the evolution of the RMSE as a function of the exponent, as well as the position of the exponent giving the minimum RMSE. The optimal exponents were distributed from ~ -1.5 to 4.5 (M, τ=1: 1.17 ± 1.1; τ_{opt}: 1.57 ± 1.12, W, τ=1: 0.94 ± 0.88; τ_{opt}: 1.59 ± 0.92). However, each minimum was surrounded by an m interval with a width at least of 1 in which the RMSE varied by less than 0.1 ms. Within these intervals, $K_1(m)$ and $K_2(m)$ often varied a hundred fold or more, due to the change of sign of m and of the convexity of the function (m > or < 1).

Besides minimizing the residue and the correlation, we also want the models to correctly predict the QT_c, which is analyzed in the next sections. A quick test to gauge if the three-parameter model should still be considered is to analyze its K_1+K_2 values, the predicted QT at RR=1000 ms. For some patients, the difference between the P^0 and the two-parameter models B^0, F^0 and P reached 15 to 20 ms, which indicated that the P^0 should be kept for QT_c analysis.

3.3. Comparison with the reference QT at 1000 ms

Comparison using $\overline{\mathrm{QTX}_c}$ *or* QTX^1

As mentioned in the methods section, $\mathrm{QT}^1_{\mathrm{ref}}$ can be compared either to QTX^1 (model X evaluated at $\overline{\mathrm{RR}} = 1$) or to $\overline{\mathrm{QTX}_c}$, the mean of the beat to beat evaluation of the QT_c. The latter can be computed using either the proportional ($QTX_{cp}(n)$, Eq. (7)) or linear scaling ($QTX_{cL}(n)$. It is shown in Appendix I that, if $\langle \varepsilon \rangle = 0$ and $\rho\left(\varepsilon(n), \overline{RR}^m(n)\right) = 0$, which is always fulfilled for the models with offset and was also found the P and P^{JT} model (c.f. Appendix II):

- $\overline{QTX_{cL}} = \overline{QTX_{cp}} = QTX^1$
- $\sigma_{QTX_{cp}} \approx \sigma_{QTX_{cL}} \Big/ \left\langle \overline{RR}^m \right\rangle$

Since $1 > m > 0$ for the all 2-parameters models as for most subjects for the P^o model, and $\left\langle \overline{RR}^m \right\rangle$ most often < 1, $\sigma_{QTX_{cp}} > \sigma_{QTX_{cL}}$ for almost all subjects, and always close to 1 for the others. The same result was found for the one parameter models. (Table A2, Fig A2 C).

Since beat-to-beat variations of the QT_c can inform us about the effect of different conditions on cardiac repolarization, the $QT_c(n)$ time series is relevant. The aforementioned conclusion ($\sigma_{QT_{cp}} > \sigma_{QT_{cL}}$,otherwise $\sigma_{QT_{cp}} \approx \sigma_{QT_{cL}}$) favored the choice $QT_{cL}(n)$ for comparison with QT^1_{ref} and extraction of potential meaningful beat-to-beat fluctuations, as proposed by Rautaharju and Zhang (2002). As shown in Appendix I, linear scaling has also an additional advantage. The correlations of $QT_{cL}(n)$ and the residues with RR^m are the same such that, as a consequence of Fig. 3, the time series $QT_{cL}(n)$ from the 2- and 3-parameter models were not correlated with RR^m. Furthermore,

$$\sigma(QTX_{cL}) = \sigma(\varepsilon - \varepsilon_o) = \sqrt{\langle \varepsilon^2 \rangle - \varepsilon_0^2} = \sqrt{RMSE^2 - \varepsilon_0^2}$$
$$\sigma(QTX_{cL} - QTX^1) = \sigma(QTX_{cL})$$

Hence, once $\overline{QTX_{cL}} - QTX^1$ is known, the variances can be obtained directly from the results of the fitting. For all models, including the one-parameter models, the linear formulation requires the data to be fitted. It is not burdensome if enough data are already available to compute optimal RR. However, the only models that could be used for brief time series would be the B, F or B^{JT} models with proportional scaling. In the next section, we compare $QT_{cL}(n)$ to QT^1_{ref}. To alleviate the notation, it is referred to simply as $QT_c(n)$.

Comparison of QTX_c *and* QT^1_{ref}

Details of the QTX_c vs QT^1_{ref} comparison are presented in Table 8

Model	**B**	**F**	**B^{JT}**	**P**	**P^{JT}**	**B^{O}**	**F^{O}**	**P^{O}**
				$\overline{QT_{cL}} - QT^1_{ref}$				
M ,τ=1	5.0 ± 6.0	-1.6 ± 4.9	1.2 ± 4.5	-2.1 ± 4.8	-2.1 ± 4.8	-2.1 ± 4.7	-2.2 ± 4.8	-2.0 ± 4.2
M τ_{opt}	5.6 ± 6.0	-1.3 ± 4.9	1.7 ± 4.5	2.4 ± 4.6	2.5 ± 4.7	2.4 ± 4.6	2.3 ± 4.5	3.1 ± 5.4
W, τ=1	7.7 ± 11.	-0.3 ± 7.8	3.8 ± 8.6	1.6 ± 6.5	1.8 ± 6.6	1.8 ± 6.7	1.5 ± 6.5	2.3 ± .5.8
W τ_{opt}	8.5 ± 11	0.2 ± 7.8	4.5 ± 8.5	7.1 ± 8.9	7.3 ± 9.2	7.1 ± 9.0	6.7 ± 8.5	9.6 ± 11.2

Table 8: $\overline{QT_{cL}}$ - QT^1_{ref} without memory and at τ_{opt}.

2- and 3-parameter models

The behavior of all 2 and 3 parameters models was identical and is illustrated by the P model in figure 6 A-D). For both men and women with mean RR < ~ 800 ms, $\overline{QTX_c}$ were overestimated for both men and women with mean RR < ~ 800 ms, the difference being amplified to reach 20 to 30 ms at τ_{opt}. The effect was larger for the P^o

model and for women. This can also be clearly seen following the position of the upper decile in fig. 7E. For subjects with mean RR > ~ 800 ms , $\langle QTX_c \rangle - QT^1_{ref}$ varied from -10 to 10 ms, with a positive correlation to mean RR without memory. This range was lessened and the correlation suppressed at τ_{opt} .

B, B^{JT} models

The B, B^{JT} models were similar to the aforementioned models, except that the results were not changed by memory. This was expected, since their parameter K_2 has been shown to be invariant with respect to memory. For subjects with mean RR > ~ 800 ms, varied between -10 to 10 ms, with no correlation to mean RR, for subjects with mean RR > ~ 800 ms, the overestimation could reach 40 ms for women.

F model

The F model brought the more interesting results. It was invariant with respect to memory due to the memory invariance of K_2. The width of the distribution of the $\langle QTX_c \rangle - QT^1_{ref}$ was similar to that of the 2 and 3 parameters models, but much more symmetrically spread with a median close to 0, without systematic bias for subject with low mean RR.

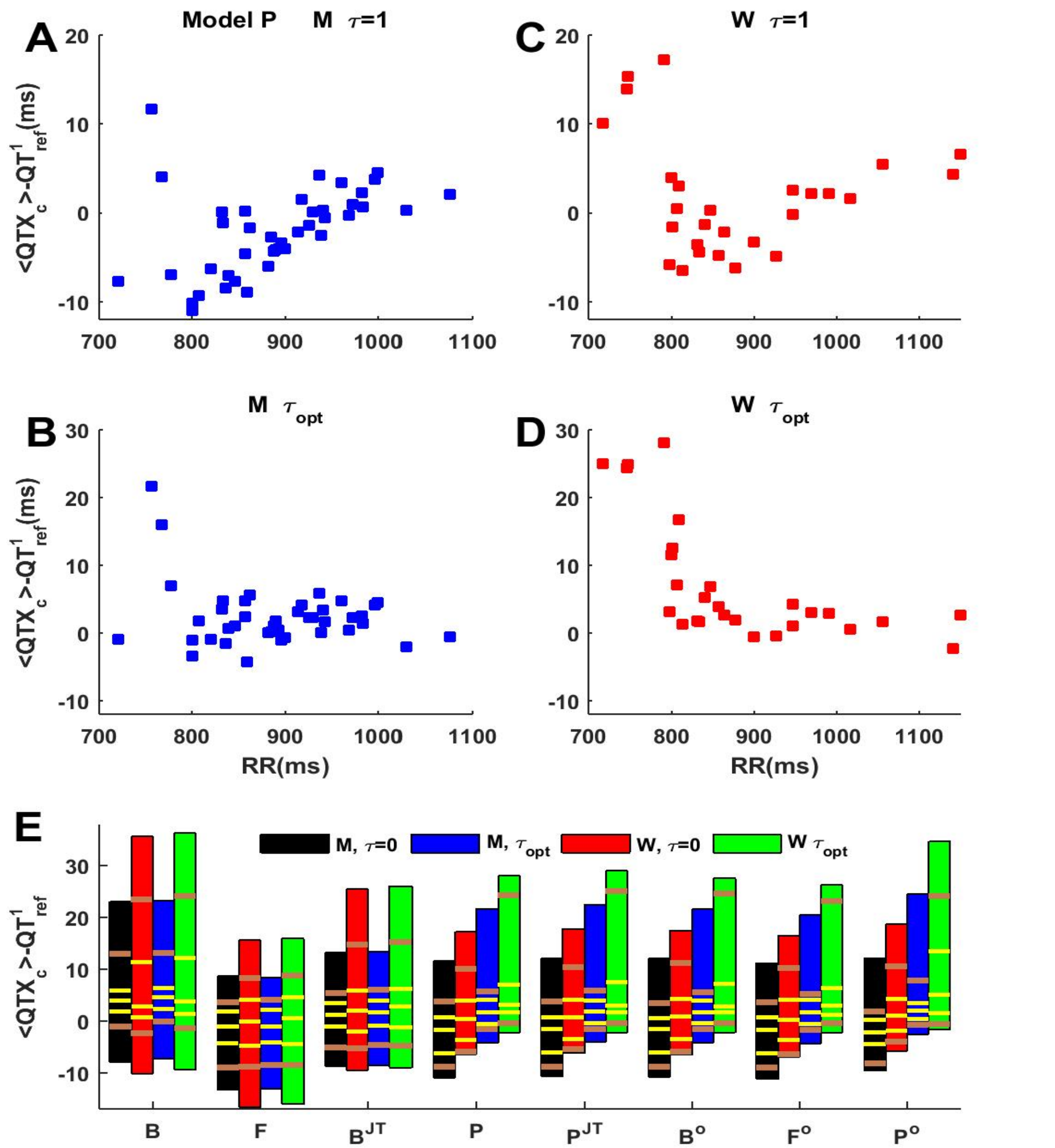

Fig 6. **A-D)** $\langle \mathrm{QTX_c} \rangle - \mathrm{QT^1_{ref}} = \overline{\mathrm{QTX_c}} - \mathrm{QT^1_{ref}}$ as a function of the mean RR values for the P model. Without memory: **A)** M, **B)** W; τ_{opt} : **C)** M , **D)** W . **E)**: Distribution of $\overline{\mathrm{QTX_c}} - \mathrm{QT^1_{ref}}$: Men, without memory (black) and with τ_{opt} (blue), Women without memory (red) and with τ_{opt} (green). The yellow lines indicate the position of the median, first and third quartile, the brown lines, the first and ninth decile.

4. Discussion

Memory reduced the RMSE of all models, thereby improving beat-to-beat QT forecast. The same optimal value could be used for all models, as well as for Men and Women. We have chosen τ_{opt} =241 beats, but the increase of RMSE was less than 0.25 ms in a range of at least 100 around τ_{opt}. Memory reduced the dispersion of the RR and increased the steepness of the QT vs. RR variation by pulling in the value of brief runs of long or short RR.

The lone parameter of the standard B and F and related B^{JT} models was invariant with respect to memory, such that improved RMSE (Fig. 1 A, B; Table 3) relied wholly on the reduction of RR dispersion. Although this stability could be clinically relevant, these models were less appropriate for fitting since they resulted in higher RMSE with a large distribution of residue vs. RR correlations (Fig. 3). However, the Fridericia model had interesting properties regarding QT_c prediction. Its $\overline{QT_C}$ were evenly spread around QT^1_{ref}, and their scattering insensitive to memory due to the invariance of its parameter (Table 6). The dispersion of its $\overline{QT_{cL}} - QT^1_{ref}$ (Fig. 6), ranging from -15 to +15 ms and evenly spread around 0, was only slightly larger than those of the two and three-parameter models without memory.

All two-parameter models (B^o, F^o, P, P^{JT}) offered proper and equivalent alternatives for fitting, reducing both the RMSE and the correlations of the residue with

$\overline{RR^m}$ (Fig. 1, 3; Tables 3). As illustrated for the P model in Fig. 4, the fitted optimal parameters were robust, meaning that any deviation from these values induced a substantial change especially for $\rho\left(\varepsilon, \overline{RR^m}\right)$ and that they had to be specific to each subject. However, they were all providing overestimated QT_c for subjects with mean RR < ~ 800 ms, their $\overline{QT_{cL}} - QT^1_{ref}$ becoming worse at τ_{opt} and being larger for women (Fig. 6). This could be explained by the slope of the QT vs RR relation, which was steeper for women and increased by memory, whereby improving the fit for data clustered at low RR led to overestimated QT at RR=1000 ms. This is further illustrated in Fig. 7, in which the data of each subject were selected over different range of RR, smaller than 900 or 800 , and then fitted to get the QT_c. Moving the RR upper limit farther from 1000 ms led to greater $\overline{QT_{cL}} - QT^1_{ref}$.

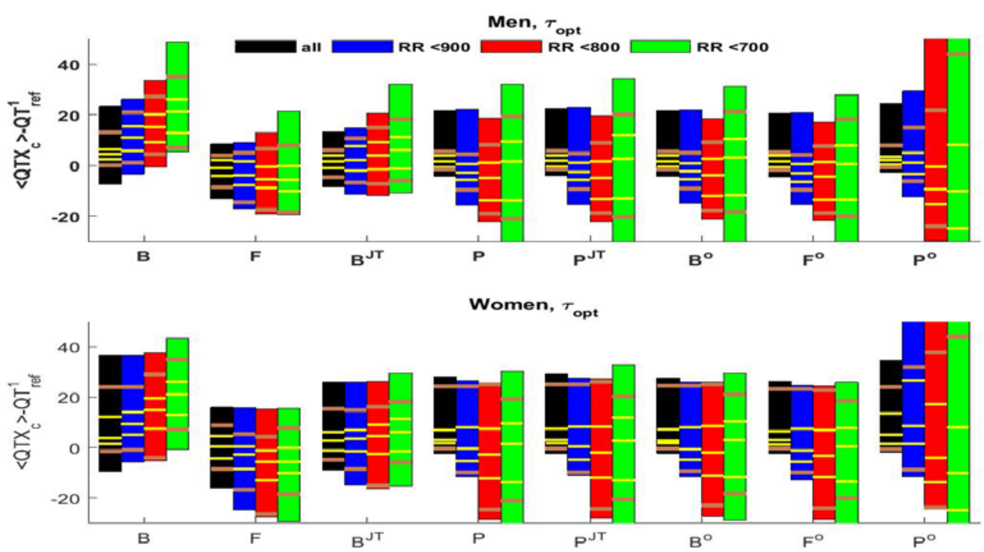

Fig. 7 Distribution of $\langle QTX_c \rangle - QT^1_{ref} = \overline{QTX_c} - QT^1_{ref}$ at τ_{opt} for Men (top) and Women (Bottom) for each model. Fitting was done using all $\overline{RR}$ (Black), or $\overline{RR}$ < 900 (Blue), < 800 (Red). < 700 (Green) ms. The yellow lines indicate the position of the median, first and third quartile, the brown lines, the first and ninth decile. Ordinate was restricted from -30 to 50 ms, and some data of P^O were beyond this interval.

Finally, the improvement of the fitting brought by three-parameter models was marginal. As shown in Fig. 5, the final optimal parameters were very sensitive since they could vary in a large range with negligible effect on RMSE and correlations. It also led to even or worse prediction of QT_c than the two-parameter models, especially at τ_{opt}.

It is noteworthy that all the characteristics of the above discussion applied to both the M and W groups. Besides, especially at τ_{opt}, the two and three-parameters models could enhance false long-QT diagnosis for subjects with low mean RR.

5. Conclusion

In term of QT_c determination, Fridericia's model was the best among the class of models that we examined and appears to be best suited for extrapolation. Its parameter was stable with respect to memory and there was no systematic trend in the difference between the predicted QT_c and the reference values. Regarding the beat-to-beat QT_c fluctuations, all two-parameter models were equivalent and appropriate, except for their capacity to correctly extrapolate the value of the QT_c for subjects with fast heart rate.

Acknowledgment

Data used for this research was provided by the Telemetric and Holter ECG Warehouse of the University of Rochester (THEW), NY. This work was supported by the Natural Sciences and Engineering Research Council of Canada [NSERC grants number RGPIN-2015-05658 to V.J. and RGPIN-2014-05558 to A.V.] and by the FRQS "Groupe de Recherche en Sciences et Technologies Biomédicales."

References

Cabasson A, Meste O & Vesin JM. (2012). Estimation and modeling of QT-interval adaptation to heart rate changes. *IEEE Trans Biomed Eng* **59,** 956-965.

Dubé B, LeBlanc A, Dutoy JL, Derome D & Cardinal R. (1988). PC-based ST-segment monitoring with the VCG. In *Engineering in Medicine and Biology Conference*, pp. 1768-1770.

Ehlert FA, Goldberger JJ, Rosenthal JE & Kadish AH. (1992). Relation between QT and RR intervals during exercise testing in atrial fibrillation. *Am J Cardiol* **70,** 332-338.

Elandt-Johnson RC & L JN. (1980). *Survival Models and Data Analysis*. John Wiley & Sons, New York.

Franz MR, Schaefer J, Schottler M, Seed WA & Noble MI. (1983). Electrical and mechanical restitution of the human heart at different rates of stimulation. *Circ Res* **53,** 815-822.

Halamek J, Jurak P, Bunch TJ, Lipoldova J, Novak M, Vondra V, Leinveber P, Plachy M, Kara T, Villa M, Frana P, Soucek M, Somers VK & Asirvatham SJ. (2010). Use of a novel transfer function to reduce repolarization interval hysteresis. *J Interv Card Electrophysiol* **29,** 23-32.

Hofman N, Wilde AA, Kaab S, van Langen IM, Tanck MW, Mannens MM, Hinterseer M, Beckmann BM & Tan HL. (2007). Diagnostic criteria for congenital long QT syndrome in the era of molecular genetics: do we need a scoring system? *Eur Heart J* **28,** 575-580.

Isbister GK & Page CB. (2013). Drug induced QT prolongation: the measurement and assessment of the QT interval in clinical practice. *British journal of clinical pharmacology* **76,** 48-57.

Jacquemet V, Cassani Gonzalez R, Sturmer M, Dube B, Sharestan J, Vinet A, Mahiddine O, Leblanc AR, Becker G, Kus T & Nadeau R. (2014). QT interval measurement and correction in patients with atrial flutter: a pilot study. *J Electrocardiol* **47,** 228-235.

Jacquemet V, Dube B, Knight R, Nadeau R, LeBlanc AR, Sturmer M, Becker G, Vinet A & Kus T. (2011). Evaluation of a subject-specific transfer-function-based nonlinear QT interval rate-correction method. *Physiol Meas* **32,** 619-635.

Malik M. (2014). QT/RR hysteresis. *J Electrocardiol* **47,** 236-239.

Malik M, Farbom P, Batchvarov V, Hnatkova K & Camm AJ. (2002). Relation between QT and RR intervals is highly individual among healthy subjects: implications for heart rate correction of the QT interval. *Heart* **87,** 220-228.

Malik M, Hnatkova K, Kowalski D, Keirns JJ & van Gelderen EM. (2013). QT/RR curvatures in healthy subjects: sex differences and covariates. *Am J Physiol Heart Circ Physiol* **305,** H1798-1806.

Malik M, Hnatkova K, Novotny T & Schmidt G. (2008a). Subject-specific profiles of QT/RR hysteresis. *Am J Physiol Heart Circ Physiol* **295,** 2356.

Malik M, Hnatkova K, Sisakova M & Schmidt G. (2008b). Subject-specific heart rate dependency of electrocardiographic QT, PQ, and QRS intervals. *J Electrocardiol* **41,** 491-497.

Malik M, Johannesen L, Hnatkova K & Stockbridge N. (2016). Universal Correction for QT/RR Hysteresis. *Drug Safety* **39,** 577-588.

Molnar J, Weiss J, Zhang F & Rosenthal JE. (1996). Evaluation of five QT correction formulas using a software-assisted method of continuous QT measurement from 24-hour Holter recordings. *Am J Cardiol* **78,** 920-926.

Pickham D, Mortara D & Drew BJ. (2012). Time dependent history improves QT interval estimation in atrial fibrillation. *J Electrocardiol* **45,** 556-560.

Pueyo E, Smetana P, Caminal P, de Luna AB, Malik M & Laguna P. (2004). Characterization of QT interval adaptation to RR interval changes and its use as a risk-stratifier of arrhythmic mortality in amiodarone-treated survivors of acute myocardial infarction. *IEEE Trans Biomed Eng* **51,** 1511-1520.

Rabkin SW & Cheng XB. (2015). Nomenclature, categorization and usage of formulae to adjust QT interval for heart rate. *World journal of cardiology* **7,** 315-325.

Rautaharju PM & Zhang ZM. (2002). Linearly scaled, rate-invariant normal limits for QT interval: eight decades of incorrect application of power functions. *Journal of cardiovascular electrophysiology* **13,** 1211-1218.

Stramba-Badiale M, Locati EH, Martinelli A, Courville J & Schwartz PJ. (1997). Gender and the relationship between ventricular repolarization and cardiac cycle length during 24-h Holter recordings. *European heart journal* **18,** 1000-1006.

Stuart A & Ord K. (1998). *Kendall's Advanced Theory of Statistics, Distribution Theory*, vol. 1. Arnold, London.

Tsai SF, Houmsse M, Dakhil B, Augostini R, Hummel JD, Kalbfleisch SJ, Liu Z, Love C, Rhodes T, Tyler J, Weiss R, Hamam I, Winner M & Daoud EG. (2014). QTc compared to JTc for monitoring drug-induced repolarization changes in the setting of ventricular pacing. *Heart Rhythm* **11,** 485-491.

Xue Q & Reddy S. (1998). Algorithms for computerized QT analysis. *J Electrocardiol* **30 Suppl,** 181-186.

Appendix I

Least square fitting of

$$y(n) = m\,x(n) + b + \varepsilon(n)$$

assures that

$$\varepsilon_o = \langle \varepsilon \rangle = 0$$
$$\langle \varepsilon, x \rangle = 0$$
$$\Rightarrow \rho(\varepsilon, x) \propto \left\langle (\varepsilon - \varepsilon_o)\left\langle x - \overline{x} \right\rangle \right\rangle = \langle \varepsilon, x \rangle - \varepsilon_o \overline{x} = 0$$

For model without the offset b, ε_o can be $\neq 0$, and $\rho(\varepsilon, x) \propto -\varepsilon_0 \overline{x}$

Consider the model:

$$\mathrm{QT_{pr}}(n) = K_1 + K_2 \cdot \overline{\mathrm{RR}(n)}^{m}$$
$$\mathrm{QT}(n) = \mathrm{QT_{pr}}(n) + \varepsilon(n)$$
$$\mathrm{QT_{pr}^{1}} = K_1 + K_2$$

where $\mathrm{QT_{pr}}(n)$ and QT(n) are the predicted and measured values respectively, $\varepsilon(n)$ the residues of the fit, $\overline{\mathrm{RR}}(n)$ the normalized and possibly autoregressive-filtered beat-to-beat interval, and $\mathrm{QT_{pr}^{1}}$ the predicted value at $\overline{\mathrm{RR}}$ =1 that is also an evaluation of the $\mathrm{QT_c}$. Using the procedure referred to as proportional scaling by Rautaharju et al. (2002), the beat-to-beat evaluation of the $\mathrm{QT_c}$ is:

$$\mathrm{QT_{cp}}(n) = \frac{\mathrm{QT}(n) - K_1}{\overline{\mathrm{RR}(n)}^{m}} + K_1 = \mathrm{QT_{pr}^{1}} + \frac{\varepsilon(n)}{\overline{\mathrm{RR}(n)}^{m}} \qquad \text{(AI.1)}$$

The fluctuations of $\mathrm{QT_{cp}}$ are an amplified with regard to $\varepsilon(n)$ if either m >0 and $\overline{\mathrm{RR}}$ <1, or m<0 and $\overline{\mathrm{RR}}$ >1.

The mean value and standard deviation are

$$\overline{\mathrm{QT}_{cp}} = \left\langle \mathrm{QT}_{cp}(n) \right\rangle = \mathrm{QT}^1_{pr} + \left\langle \frac{\varepsilon(n)}{\overline{\mathrm{RR}(n)}^{m}} \right\rangle \qquad \text{(AI.3)}$$

$$\sigma\left(\mathrm{QT}_{cp}\right) = \sigma\left(\frac{\varepsilon(n)}{\overline{\mathrm{RR}(n)}^{m}} \right) \qquad \text{(AI.4)}$$

If ε and $\overline{\mathrm{RR}}^{m}$ are normally distributed, with $\langle \varepsilon \rangle = \varepsilon_o$ and $\left\langle \overline{\mathrm{RR}}^{m} \right\rangle = \mathrm{A}$ with correlation coefficient ρ, they can be approximated as (Elandt-Johnson & L, 1980; Stuart & Ord, 1998) :

$$\left\langle \frac{\varepsilon(n)}{\overline{\mathrm{RR}(n)}^{m}} \right\rangle \approx \frac{\varepsilon_o}{\mathrm{A}} + \frac{\varepsilon_o\, \sigma\left(\overline{\mathrm{RR}(n)}^{m}\right)^2}{\mathrm{A}^3} - \frac{\rho\, \sigma\left(\overline{\mathrm{RR}(n)}^{m}\right)\sigma(\varepsilon)}{\mathrm{A}^2} \qquad \text{(A1.5)}$$

$$\sigma\left(\mathrm{QT}_{cp}\right)^2 \approx \frac{\sigma(\varepsilon)^2}{\mathrm{A}^2} - 2\frac{\varepsilon_o}{\mathrm{A}^3}\rho\, \sigma\left(\overline{\mathrm{RR}(n)}^{m}\right)\sigma(\varepsilon) + \frac{\varepsilon_o^2}{\mathrm{A}^4}\sigma\left(\overline{\mathrm{RR}(n)}^{m}\right)^2 \qquad \text{(A1.6)}$$

Hence, if ε unbiased (i.e. $\varepsilon_o = 0$) and $\rho = 0$, as in models with offset,

$$\overline{\mathrm{QT}_{cp}} \approx \mathrm{QT}^1_{pr} \qquad \text{(A1.7)}$$

$$\sigma\left(\mathrm{QT}_{cp}\right) \approx \frac{\sigma(\varepsilon)}{\mathrm{A}} = \frac{\mathrm{RMSE}}{\mathrm{A}} \qquad \text{(A1.8)}$$

Otherwise $\sigma(\varepsilon)^2 = \mathrm{RMSE}^2 - \varepsilon_0^2$.

An alternative approach to calculate $\mathrm{QT}_c(n)$, termed linear scaling by Rautaharju et al. (2002), is:

$$\mathrm{QT}_{cL}(n) = \left(\mathrm{QT}(n) - \mathrm{K}_2 \cdot \overline{\mathrm{RR}(n)}^{m}\right) + \mathrm{K}_2 = \mathrm{QT}^1_{pr} + \varepsilon(n)$$

Then

$$\overline{\mathrm{QT}_{cL}} = \left\langle \mathrm{QT}_{cL} \right\rangle = \mathrm{QT}^1_{pr} + \varepsilon_o \qquad \text{(A1.9)}$$

$$\sigma^2_{\mathrm{QT}_{cL}} = \sigma^2_{\varepsilon} = \left\langle \left(\varepsilon(n) - \varepsilon_o\right)^2 \right\rangle = \mathrm{RMSE}^2 - \varepsilon_o^2 \qquad \text{(A1.10)}$$

Then, by AI.3, AI.7:

$$\overline{QT_{cp}} - \overline{QT_{cL}} = \left\langle \frac{\varepsilon}{\overline{RR}^{m}} \right\rangle - \varepsilon_o \qquad \text{(AI.11)}$$

which, by AI.5, can be approximated by

$$\overline{QT_{cp}} - \overline{QT_{cL}} \approx \varepsilon_o \left(\frac{1}{A} - 1 \right) + \frac{\varepsilon_o \, \sigma\left(\overline{RR(n)}^{m} \right)^2}{A^3} - \frac{\rho \, \sigma\left(\overline{RR(n)}^{m} \right) \sigma(\varepsilon)}{A^2} \qquad \text{(AI.12)}$$

If ε unbiased and $\rho = 0$, $\overline{QT_{cp}} \approx \overline{QT_{cL}}$

By AI.4 and AI.10,

$$\frac{\sigma(QT_{cp})}{\sigma(QT_{cL})} = \frac{\sigma\left(\frac{\varepsilon}{\overline{RR}^{m}} \right)}{\sigma(\varepsilon)} \qquad \text{(AI.13)}$$

which, by AI.6, can be approximated by

$$\frac{\sigma(QT_{cp})^2}{\sigma(QT_{cL})^2} \approx \frac{1}{A^2} - 2 \frac{\varepsilon_o}{A^3} \frac{\rho \, \sigma\left(\overline{RR(n)}^{m} \right)}{\sigma(\varepsilon)} + \frac{\varepsilon_o^2}{A^4} \frac{\sigma\left(\overline{RR(n)}^{m} \right)^2}{\sigma(\varepsilon)^2} \qquad \text{(AI.14)}$$

If the mean of $RR^m < 1$, without bias $(\varepsilon_o \to 0)$ and correlation $(\rho \to 0)$, $\sigma_{QT_{cp}} > \sigma_{QT_{cL}}$

Appendix II

II.1 Comparison of $\mathrm{QTX_{cL}}$ and $\mathrm{QTX_{cp}}$

By definition

$$\overline{\mathrm{QTX_{cp}}} = \mathrm{QTX^1_{pr}} + \left\langle \frac{\varepsilon(n)}{\overline{\mathrm{RR(n)}}^{m}} \right\rangle$$

$$\overline{\mathrm{QTX_{cL}}} = \langle \mathrm{QTX_{cL}} \rangle = \mathrm{QTX^1_{pr}} + \varepsilon_o$$

$$\sigma(\mathrm{QTX_{cp}}) = \sigma\left(\frac{\varepsilon(n)}{\overline{\mathrm{RR(n)}}^{m}} \right)$$

$$\sigma^2_{\mathrm{QTX_{cL}}} = \sigma^2_{\varepsilon} = \left\langle (\varepsilon(n) - \varepsilon_o)^2 \right\rangle = \mathrm{RMSE}^2 - \varepsilon_o^2$$

According to approximation AI.12, $\left\langle \varepsilon / \overline{\mathrm{RR}}^{m} \right\rangle \to 0$ if ε_o and $\rho\left(\varepsilon, \overline{\mathrm{RR}}^{m}\right) \to 0$, whereby $\overline{\mathrm{QTX_{cp}}} \approx \overline{\mathrm{QTX_{cL}}} \approx \mathrm{QTX^1_{pr}}$. By construction, these two conditions are always fulfilled by models with offset. Both conditions were also found to be realized for the P and $\mathrm{P^{JT}}$ models ($\rho\left(\varepsilon, \overline{\mathrm{RR}}^{m}\right) \approx 0$ Fig, 3, Table 5, $\varepsilon_o \approx 0$, Fig. A2 A and B).

For B and $\mathrm{B^{JT}}$ models without memory, ε_o could be up to 3 ms and $\overline{\mathrm{QTX_{cp}}} - \overline{\mathrm{QTX_{cL}}} > 0$, but both quantities were reduced at τ_{opt}. They were smaller for the F model, the median being always close to 0 for the two groups and two memories. These small differences did not provide a convincing argument to select either $\mathrm{QT_{cL}}$ or $\mathrm{QT_{cp}}$.

However, for most subjects $\sigma(QTX_{cP})$ was larger than $\sigma(QTX_{cL})$ (Fig. A2 C, Table A2). The few cases where $\sigma(QTX_{cP}) < \sigma(QTX_{cL})$ had $\left\langle \overline{RR}^{m} \right\rangle > 1$, a result consistent with eq. A1.12. The P^0 model had the largest $\sigma(QT_{cP})/\sigma(QT_{cL})$ spread, resulting from its wide range exponents (Fig. 5) since $\sigma(QTP^{o}{}_{cP})/\sigma(QTP^{o}{}_{cL}) \approx 1/\left\langle \overline{RR}^{m} \right\rangle$ in this model

$\frac{\sigma(QT_{cP})}{\sigma(QT_{cL})}$	**B**	**F**	**B^{JT}**	**P**	**B^{O}**	**F^{O}**	**P^{JT}**	**P^{0}**
τ=1, M	1.11 ± 0.05	1.06 ± 0.03	1.10 ± 0.05	1.05 ± 0.03	1.06 ± 0.04	1.09 ± 0.05	1.06 ± 0.03	1.31 ± 0.41
τ=1 ,W	1.10 ± 0.07	1.05 ± 0.04	1.09 ± 0.07	1.06 ± 0.05	1.08 ± 0.06	1.09 ± 0.07	1.06 ± 0.05	1.22 ± 0.29
% >1 M **W**	98 89	98 89	98 89	98 89	98 89	98 89	98 89	83 70
τ_{opt} **,M**	1.10 ± 0.05	1.04 ± 0.03	1.08 ± 0.05	1.06 ± 0.04	1.08 ± 0.05	1.08 ± 0.05	1.05 ± 0.03	1.40 ± 0.45
τ_{opt} **,W**	1.09 ± 0.07	1.05 ± 0.05	1.08 ± 0.07	1.08 ± 0.07	1.10 ± 0.08	1.08 ± 0.07	1.05 ± 0.05	1.36 ± 0.42
% >1 M **W**	95 85	93 85	93 85	95 85	95 85	95 85	95 85	95 85

Table AII.1. Distribution of $\sigma(QT_{cP})/\sigma(QT_{cL})$ without memory and at τ_{opt} in both groups. The third and sixth lines give the % of subjects for which $\sigma(QT_{cP})/\sigma(QT_{cL}) > 1$.

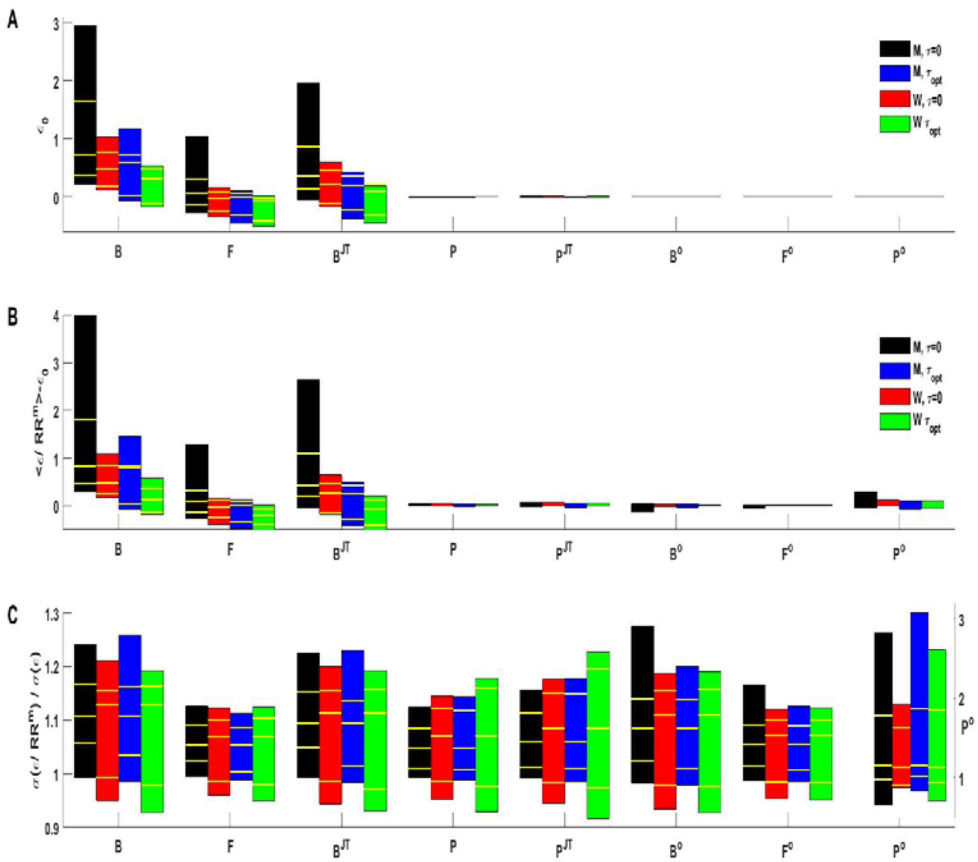

Fig. A2. Men, without memory (black) and with τ_{opt} (blue), Women without memory (red) and with τ_{opt} (green). The yellow lines indicate the position of the median, first and ninth decile. For each model, distribution of **A**: ε_o (ms) ; **B**: $\left\langle \varepsilon / \overline{RR}^m \right\rangle - \varepsilon_o$; **C**: $\sigma\left(\varepsilon / \overline{RR}^m\right) / \sigma(\varepsilon)$. In this last panel, the ordinate left scale applies to all models except P^o, whose scale appears on the right.